Audio Engineering Society

# Convention Paper

Presented at the 129th Convention
2010 November 4–7 San Francisco, CA, USA



# Contributions to the improvement of the response of a Pleated Loudspeaker

Martínez, J.[1], Martínez, R.[1], Segovia, E.[2], Carbajo, J.[3] and Ramis, J.[3]

[1] Acústica Beyma S.L., Moncada, Valencia, 46113, Spain
j.martinez@beyma.com

[2] Dpto. Ingeniería de la Construcción, Obras Públicas e Infraestructura Urbana
enrique.gonzalo@ua.es

[3] Dpto. Física, Ingeniería de Sistemas y Teoría de la Señal, San Vicente Raspeig, Alicante, 03080, Spain
jesus.carbajo@ua.es, jramis@ua.es

## ABSTRACT

In this paper we describe some results that have led to the improvement of the response of an Air Motion Transformer loudspeaker. First, it is noteworthy that it has been found an approximate analytical solution to the differential equations system that governs the behavior of the moving assembly of this type of transducer, being this valid when the length of the pleat is much greater than the radius of the cylindrical part. This solution is valid for any type of analysis (static, modal and harmonic), and the modes are significantly simplified assuming the hypothesis above mentioned. In addition, we have analyzed the influence of the thickness and the shape of perforation of the pole piece in the frequency response of the loudspeaker.

## 1. INTRODUCTION

In this paper we describe some results that have led to the improvement of the response of an Air Motion Transformer (AMT) loudspeaker.

This work was developed in the context of research into optimizing the frequency response of an Air Motion Transformer loudspeaker – AMT onwards – with a pleated moving assembly like the one shown in Figure 1 A description of this type of speaker can be found at [1] and [2]. A numerical model is presented in [3].

Theses results can be grouped into two blocks: a) that refers to the structural behavior of the moving assembly and b) about the influence and contribution of peripheral elements, particularly the pole piece, in the frequency response of this type of loudspeaker.

Figure 1 Moving assembly and polar piece of a pleated loudspeaker

With regard to the first block, it is noteworthy that it has been found an approximate and relatively "simple" analytical solution to the differential equations system that governs the dynamic behavior of the moving assembly of this loudspeaker (the dimensions have been taken according to commercial products). The approximate character is due to the fact that a simplification of the differential equations has been carried out, being this valid when the length of the loudspeaker is much greater than the radius of the cylindrical part of the pleats. The analytical expressions for the average surface displacement in any structural analysis (modal or harmonic), are considerably simplified by assuming the hypothesis above, being able to write as Levy type Fourier series, being the axial coordinate the one to which series expansion is applied.

By means of this analytical model we can easily obtain two practical results. First of them is the determination of the fundamental mode that is related to the beginning of the useful response of the loudspeaker. Secondly, the frequency corresponding to the main mode depends roughly linearly with the thickness of the base material of the moving assembly.

To test the implemented analytical model, numerical experiments in FEM (using the software Ansys©) have been developed. It was found that the first natural frequency of the moving assembly (for exciting harmonic loads, i.e. those corresponding to more excited modes with those loads) obtained with this approach differ by less than 1% of that obtained in the FEM with Ansys©. In addition, a great similarity in the modes of vibration is observed. Moreover, we have analyzed and we have given an explanation to the effect of considering that the folds in the direction of radiation are narrower (smaller radius) than those that radiate to the back.

Concerning second block, the one regarding to the acoustical component, several simulations have been carried out using the Finite Difference Time Domain Method (FDTD), to explain the influence of small variations in the thickness and the shape of the pole piece in the frequency response curve of the loudspeaker and the realization of a bevel on this part. The results of numerical experiments are confirmed with experimental measurements performed in anechoic chamber.

To approach slightly to the operation of this type of loudspeaker, Figure 2 shows the typical frequency response curve of this type of loudspeaker. As it can be marked out, the useful range starts above 1200 Hz.

On the other hand, Figure 3 shows the measured electrical impedance, where a small resonance can be appreciated around 1500 Hz.

The interest of the first part of this work lies in the possibility of predicting the effect of small changes in geometry and the characteristics of the materials that compose the moving assembly in the frequency response curve and the electrical impedance curve of the loudspeaker, without having to resort to numerical methods.

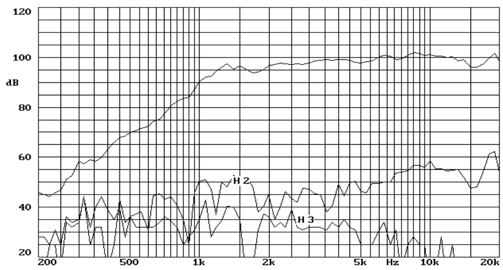


Figure 2 Frequency response of TPL-150 loudspeaker

.

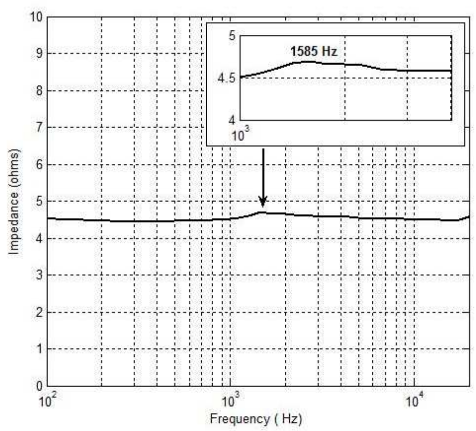


Figure 3 Total electrical impedance of TPL-150

## 2. ANALYTICAL MODEL

It is beyond the aim of this paper an exhaustive description of the methodology for carrying out a modal analysis. For a complete description of this methodology see [4 ]. This section explains the basics of the method (sections 2.1 and 2.2), discussing the results of the model implementation corresponding to a numerical experiment in FEM (2.3) and explaining a possible procedure to obtain the mechanical resonance frequency shown in the electrical impedance curve (2.4).

Like any type of acoustic transducer, its operation involves the interaction between fluid and structure. This paper presents an analytical methodology to determine their modal behaviour, focusing on the structural part. The results will be useful not only to explain the operation of these loudspeakers, but for other structures with similar geometry.

We are interested in obtaining an approximate analytical solution to the structural problem of calculating the natural frequencies and vibration modes for a structure consisting of an arbitrary sequence of plates and cylindrical panels connected by straight edges similar to the one shown in Figure 4. To approach the structural problem, we elected to start from a setting like the one shown in Figure 4, which shows a cross-section divided into five domains (I, II, III, and IV lower and IV upper). The domains I, II and III consist of a single layer of $e_1$ thickness while the other two have two layers of $e_1$ and $e_2$ thicknesses respectively. Material corresponding to layers $e_1$ (*Material 1*) and $e_2$ (*Material 2*) are different between them, being both elastic and homogeneous.

### 2.1. Governing Equations

The solution obtained in the next section builds on Classic Shell Theory (hereafter CST), assuming that thin sheets are handled and neglecting the shear strain. The differential equations of equilibrium for a circular cylindrical shell [5, 6] as applied to an open cylindrical shell of length L, radius R and subjected to an arbitrary surface load P are:

$$
\begin{aligned}
&\frac{\partial N_{xy}}{\partial y}+\frac{\partial N_x}{\partial x}=-P_x+I_1\ddot{u}-I_2\frac{\partial \ddot{w}}{\partial x}\\
&\frac{\partial N_y}{\partial y}+\frac{\partial N_{xy}}{\partial x}-\frac{Q_y}{R}=-P_y+I_1\ddot{v}-I_2\frac{\partial \ddot{w}}{\partial y}\\
&\frac{N_y}{R}+\frac{\partial Q_y}{\partial y}+\frac{\partial Q_x}{\partial x}=-P_z+I_1\ddot{w}\\
&-Q_x+\frac{\partial M_{xy}}{\partial y}+\frac{\partial M_x}{\partial x}=I_2\ddot{u}-I_3\frac{\partial \ddot{w}}{\partial x}\\
&-Q_y+\frac{\partial M_y}{\partial y}+\frac{\partial M_{xy}}{\partial x}=I_2\ddot{v}-I_3\frac{\partial \ddot{w}}{\partial y}
\end{aligned}
\qquad (1)
$$

where ($u$, $v$, $w$) are the displacements along the $x$ (axial), $y$ (circumferential) and $z$ (radial) axes respectively; the superimposed dot denoting time derivative, $P_x$, $P_y$, $P_z$ are the external force applied to the surface, $R$ is the radius of curvature and $N_i$, $M_i$, $Q_i$ are the resultant stresses (Fig. 5).

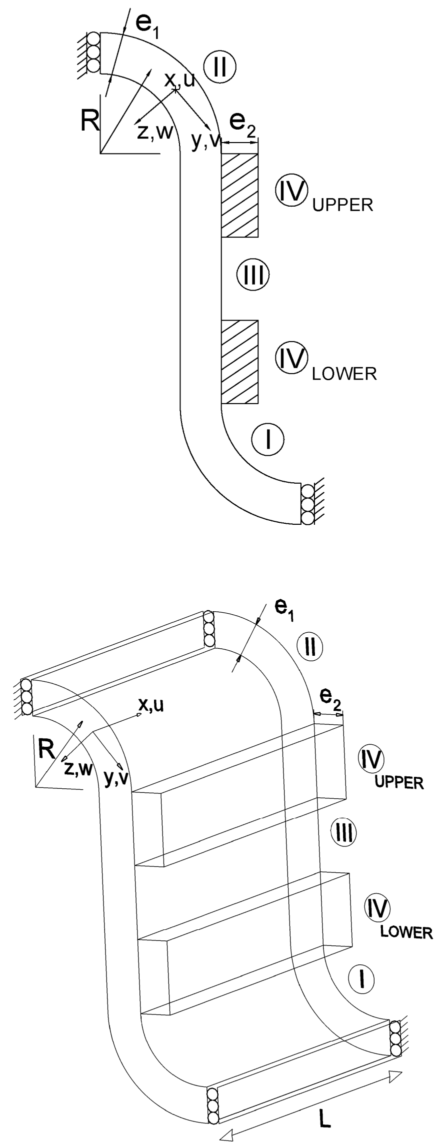


Figure 4. Example of a structure composed of plates and cylindrical panels attached by their straight sides, lateral view (Up) and three-dimensional view (Down).

$$(N_i, M_i) = \sum_{k=1}^{N} \int_{t_{k-1}}^{t_k} \sigma_i^{(k)}(1, z)dz \quad \left(i \ = \ x, \ y, \ xy\right)$$

$$(Q_x, Q_y) = \sum_{k=1}^{N} \int_{t_{k-1}}^{t_k} (\sigma_{xz}^{(k)}, \sigma_{yz}^{(k)})dz$$

The inertias $I_i$ are defined by the equations:

$$(I_1, I_2, I_3) = \sum_{k=1}^{N} \int_{t_{k-1}}^{t_k} \rho^{(k)}(1, z, z^2)dz \qquad (3)$$

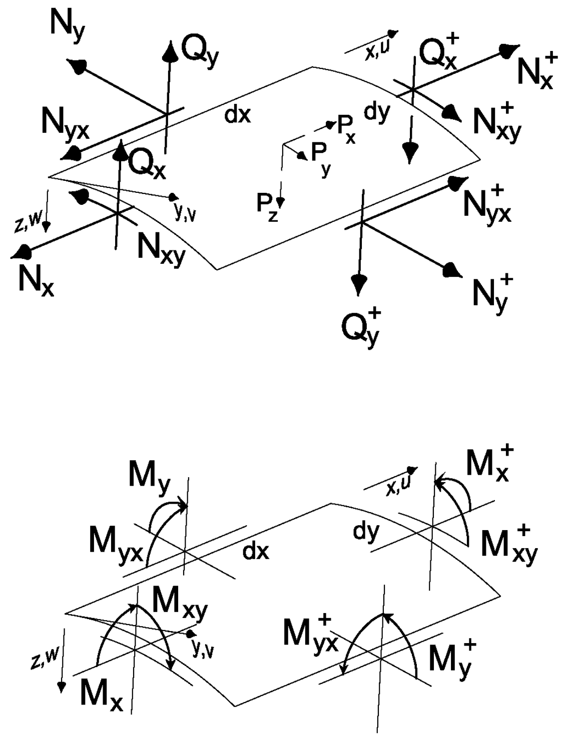

Figure 5. Axes, applied load and resultant stresses for membrane (upper) and bending (lower).

Although the term $\frac{Q_y}{R}$ in equations (1) that usually is negligible, we will use the full equation in order to have some information about the goodness of the assumptions that we will propose to develop the analytical solution.

Moreover, the resultant stresses are related to the strains by the laminate constitutive equations:

$$\begin{aligned} N_i &= A_{ij}\varepsilon_j^0 + B_{ij}k_j \\ M_i &= B_{ij}\varepsilon_j^0 + D_{ij}k_j \end{aligned} \quad \left(i, \ j \ = x, \ y, \ xy\right) \qquad (4)$$

where $A_{ij}$, $B_{ij}$, $D_{ij}$ are the laminate rigidities:

$$\left(A_{ij}, B_{ij}, D_{ij}\right) = \sum_{k=1}^{N} \int_{t_{k-1}}^{t_k} E_{ij}(1, z, z^2)dz \;\; (i,\, j \;=\; x,\; y,\; xy) \quad (5)$$

Using $A_{ij}$, $B_{ij}$, $D_{ij}$ the stress-resultant displacement relations can be deduced (see [4]

The governing equations (1) can be expressed in terms of the displacement and, in matrix form, as:

$$[L]\{\Delta\} = -P \quad (6)$$

Where:

$$\{\Delta\}^T = \{u, v, w\} \quad (7)$$

The $L_{ij}$ coefficients are listed in [4]. The reader has to notice that on these coefficients all the terms are included. On this way, the comparison between numerical and analytical results that will be carried out in a further section will highlight the accuracy of the proposed method.

Focusing on the structural problem, the main objective of this work is to find an analytical solution to structures composed of plates and cylindrical panels attached by their straight sides with the following boundary conditions:

- Arbitrary at both straight final sides.
- Hinge type at the two curved edges $x = 0$ and $x = L$: $M_x = u = v = w = 0$

Where L is the panel length (length of the straight sides). Concerning to the internal boundaries between domains, continuity conditions have to be applied.

To find the analytical solution we will use a Levy type solution, which has the general form:

$$u(x, y) = \sum_{m=1}^{\infty} f_u(y) Sin\left(\frac{m\pi x}{L}\right)$$
$$v(x, y) = \sum_{m=1}^{\infty} f_v(y) Sin\left(\frac{m\pi x}{L}\right) \quad (8)$$
$$w(x, y) = \sum_{m=1}^{\infty} f_w(y) Sin\left(\frac{m\pi x}{L}\right)$$

A solution to a similar buckling problem is available in the literature [7] if the boundary conditions are:

- Arbitrary at both straight sides.
- Simply supported at the two curved edges $x = 0$ and $x = L$: $M_x = N_x = v = w = 0$

However, no solution has been found in the available literature for the proposed boundary conditions, i.e. $u = 0$ instead of $N_x = 0$ on curved sides.

### 2.2. Proposed Method

The problem is addressed through:

$$\frac{\partial u(x, y, t)}{\partial x} << \frac{\partial v(x, y, t)}{\partial y} \quad (9)$$

For single cylindrical panels, this means that the wavelength in *x* direction is much higher than in *y* direction, which is true for a lot of vibrations modes when the length of the curved side (which has the same order of magnitude as the radius) is much smaller than the length of the straight sides. However, there are some vibration modes in which this assumption can not be made, i.e. panel with free straight sides or when there are lots of half-waves in *x*-direction and a few in *y*-direction.

Moreover, for cylindrical panels with $B_{ij} = 0$, the term $\frac{1}{R}\frac{\partial v}{\partial y}$ is part of the curvature and therefore the simplification carried out in (9) is reinforced. This may happens for this kind of panels because the membrane energy is much lower than the bending energy. For panels with $B_{ij} \neq 0$, i.e. with non symmetrical layers, the assumption made in (9) can still be used because, for this kind of panels, the strains are on the same order than the curvature multiplied by its thickness.

It may occur, as in the example application of this paper, that the simplification is not useful in some plate domain. But, if this has symmetrical layers ($B_{ij} = 0$), calculate the *w* component of movement and the natural frequency by Rayleigh method is still possible due to the membrane energy – which only depends on *u* and *v* – is much lower than the bending energy – which only depends on *w* – and, besides, the simplifications done do not involve the *w* component of the movement.

On the other hand, the structure we are working with is composed of domains with the straight part much longer than the curved one. For this kind of domain if $P_x = 0$, the assumption (9) is better fulfilled. With these considerations, equation (6) can be rewritten as:

$$\begin{pmatrix} L_{11} & L_{12} & L_{13} \\ 0 & L_{22} & L_{23} \\ 0 & L_{32} & L_{33} \end{pmatrix} \begin{Bmatrix} u(x,y,t) \\ v(x,y,t) \\ w(x,y,t) \end{Bmatrix} = \begin{Bmatrix} 0 \\ -P_y(y,t) \\ -P_z(y,t) \end{Bmatrix} \quad (10)$$

With the considered boundary conditions described above for this study, equation (10) has an analytical solution. To find this analytical solution, we use a Levy type solution, which has the general form given in (8), where the functions $f_u(y),\ f_v(y)$ and $f_w(y)$ are obtained from the solution of an ordinary differential equations system with constant coeficients.

From this point we will work with a model with a continuous mid-surface in all the domains. To do that, parts number IV have been moved in z direction. With this modification, the structure shown in figure 1 becomes that shown in figure 7, in which the reader can note that the mid-surface is continuous.

The simultaneous equations (10) will be solved in two parts: in the first part we will obtain the values of *v(x, y, t)* and *w(x, y, t)* and in the second part the value of *u(x, y, t)* will be obtained. The solution developed is similar to this that in [8].

The second and third equations from (10) are:

$$\begin{pmatrix} L_{22} & L_{23} \\ L_{32} & L_{33} \end{pmatrix} \begin{Bmatrix} v(x,y,t) \\ w(x,y,t) \end{Bmatrix} = \begin{Bmatrix} -P_y(y,t) \\ -P_z(y,t) \end{Bmatrix} \quad (11)$$

Equation (11) can be solved through:

$$\begin{aligned} v(x,y,t) &= v^c(x,y,t) + v^p(x,y,t) \\ w(x,y,t) &= w^c(x,y,t) + w^p(x,y,t) \end{aligned} \quad (12)$$

This solution consists of two parts, namely complementary function and particular integral. These two parts should be combined to obtain the overall solution. However, as we are interested in performing a modal analysis, we only need to solve the complementary function of the solution, which can be written as:

$$\begin{pmatrix} L_{22} & L_{23} \\ L_{32} & L_{33} \end{pmatrix} \begin{Bmatrix} v^c(x,y,t) \\ w^c(x,y,t) \end{Bmatrix} = \begin{Bmatrix} 0 \\ 0 \end{Bmatrix} \quad (13)$$

The accuracy of the solution obtained should be verified using equation (9).

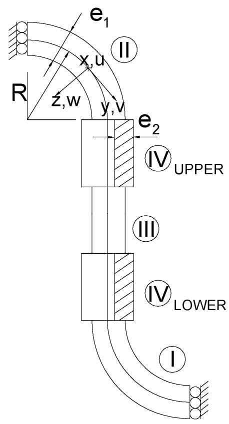


Figure 7: Example structure with the modification to have a continuous mid-surface

For a particular $m = m_0$, the natural modes have the form:

$$\begin{aligned} &v_{i,m_0}(x,y,t) = \\ &Sin(\Omega t) Sin\left(\frac{m_0 \pi x}{L}\right) * \\ &*\left(\left(g_6 d_y^3 - g_8 d_y\right) \varphi_{i,m_0}\left(y, C^i_{1m_0}, C^i_{2m_0}, C^i_{3m_0}, C^i_{4m_0}, C^i_{5m_0}, C^i_{6m_0}\right)\right) \\ &w_{i,m_0}(x,y,t) = Sin(\Omega t) * \\ &Sin\left(\frac{m_0 \pi x}{L}\right) * \\ &*\left(\left(g_1 d_y^2 - g_2\right) \varphi_{i,m_0}\left(y, C^i_{1m_0}, C^i_{2m_0}, C^i_{3m_0}, C^i_{4m_0}, C^i_{5m_0}, C^i_{6m_0}\right)\right) \end{aligned} \quad (14)$$

Where $C^i_{1m_0}$ are arbitrary constants obtained from boundary conditions and gi are listed in [ 4 ]

### 2.3. Model Validation

In order to verify the validity of the proposed method a Finite Element Model (FEM) has been implemented, by using the software Ansys 8.1. Referring to Figure 5, the geometrical data of the average surface are:

- Cylindrical panel ratio: R=0.65 mm
- Height of domains IV: 1.2 mm
- Height of domain III: 0.96 mm

- Length of the straight sides: L=125 mm

The material characteristics are:

| | Material 1 | Material 2 |
|---|---|---|
| Elastic modulus (GPa) | 3 | 127 |
| Poisson coefficient | 0.33 | 0.345 |
| Density (kg/m$^3$) | 1400 | 8900 |
| Thickness (μm) | 25 | 17 |

Table 1 Materials characteristic (1 is the base material, 2 is the reinforcement material).

These measures and mechanical characteristics correspond to a real moving assembly of a commercial loudspeaker.

In this FEM we have used a SHELL 181 element type which has six degree of freedom per node and satisfies the first order shear deformation theory. Large shear rigidity has been added in order to neglecting the deformation associated to this variable. Mapped meshing and Modal Analysis have been used. Due to the symmetry of the problem, only a half part has been modelled. Once meshed, the model is composed by 545250 elements and 545218 nodes.

The implemented model details are shown in Figure 8. Meshing and domain IV details can be appreciated:

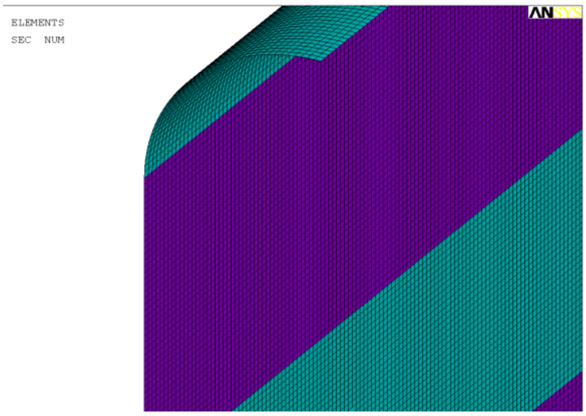


Figure 8 Meshing details

There have also been developed two versions of the analytical model described in Section 3, AM1 and AM2, both with Mathematica 4.0. In AM1 version, the term $\frac{Q_y}{R}$ and the symmetrical terms have been neglected while none has been neglected in the AM2 version. In addition, we have compared the results with and without considering Rayleigh's Method. Results for natural frequencies are compared in Table 2 for first mode with $m_0 = 1$. We have used only five summations in the Fourier series expansion for the *u* component.

| METHOD | $f_0$ (Hz) |
|---|---|
| FEM (ANSYS) | 990.1 |
| AM1 (Mathematica whitout Rayleigh's Method) | 1112.1 |
| AM1 (Mathematica with Rayleigh's Method) | 1002.8 |
| AM2 (Mathematica whitout Rayleigh's Method) | 1011.7 |
| AM2 (Mathematica with Rayleigh's Method) | 990.8 |

Table 2. First modal frequency for each one of the models implemented

Figure 9 represents the mode shapes for the fundamental mode. The results similarity can be appreciated.

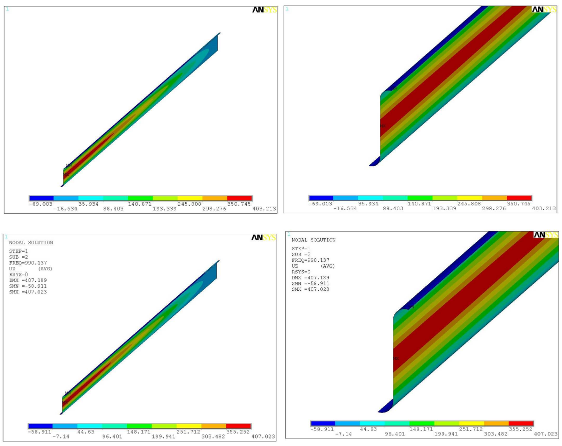

Figure 9. Comparative of the *w* component for the first mode shape; upper: AM2; lower: FEM; left: general view, right: detail view.

Finally, the results obtained with the numerical experiment and analytical model for the $f_w(y)$ of the displacement component *w* are compared in

Figure 10. To make this comparison a normalization of $f_w(y)$ has been done through establish a maximum kinetic energy of 1 both in FEM and in AM2. As can be seen, they are practically coincident:

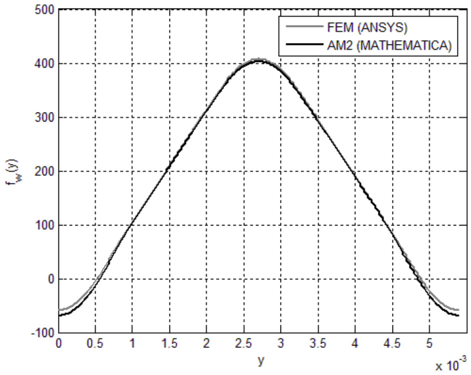


Figure 10. Comparison between analytical and numerical results of $f_w(y)$.

### 2.4. Mechanical Resonance

Although not the aim of this work, there should be noted that for calculating the approximate mechanical resonance frequency that determines the peak in the impedance curve, one option would be the next one. To determine:

a) The components u, v and w of the first mode shape from any of the models AM1 or AM2 (or with a FEM Model)

b) The maximum strain energy in this vibration mode (structural)= $E_s$

c) The average displacement of $w$ .=D

d) The acoustic energy (related with the air deformation strain) by using the equation

$$E_A = \frac{1}{2} K_A D^2$$

$$K_A = \frac{\rho_0 c^2 S^2}{V}$$

e) Finally, the frequency $f_r = \frac{1}{2\pi}\sqrt{\frac{E_S + E_A}{E_C}}$ (Previously, we have normalized the maximum kinetic energy)

For the geometry described above it has been obtained a result of 1532 Hz, very close to the experimental one shown in the Figure 3)

## 3. POLAR PIECE ACOUSTIC CONTRIBUTION

The front polar piece figs 1 and 11,, forming part of the magnetic system, contributes to the frequency response of the loudspeaker. From the acoustic point of view is like a perforated plate. In room acoustics, where the acoustic measurements of interest are up to 4 kHz, perforated plates with a drilling rate of over 25% are considered transparent to sound. However, in the area where we are, we are dealing with systems that radiate higher frequencies sound and the effect of that piece is felt.

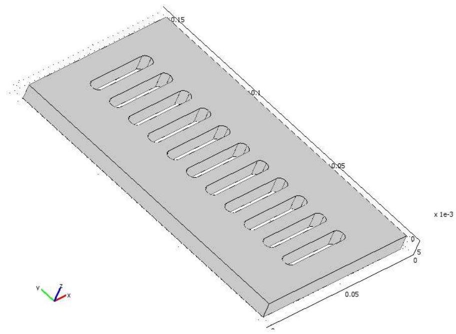

Figure 11 Front polar piece

In a first approach to the problem, there have been carried out several numerical experiments, implementing several simulations by using FDTD and FEM that are methods well know and usually used in the acoustic and electromagnetic context (see i.e.[8,9,10])

Although being different methods, models reflect the same pattern.

Trying to simulate anechoic conditions, Perfectly Matched Layers (PMLs) have been applied to the models as it can be seen in Figure 12 and 13. The measurement point is placed 0.5 m from the loudspeaker, trying to simulate the experimental measurement conditions. Source was simulated as a flat piston with the same dimensions as those of the moving assembly.

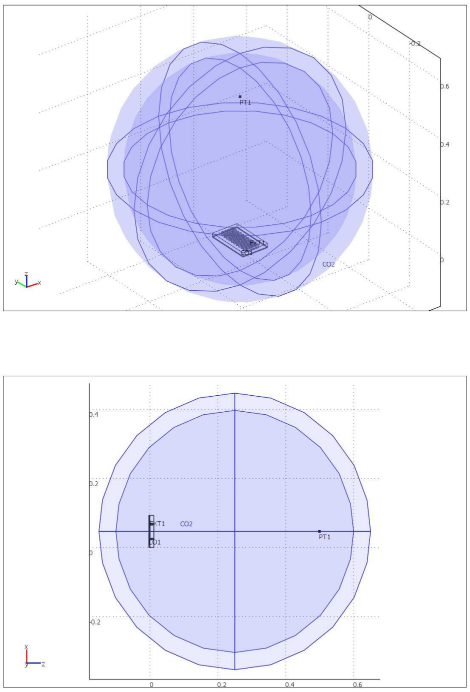

Figure 12 Model with Perfect Matched Layers (PMLs)

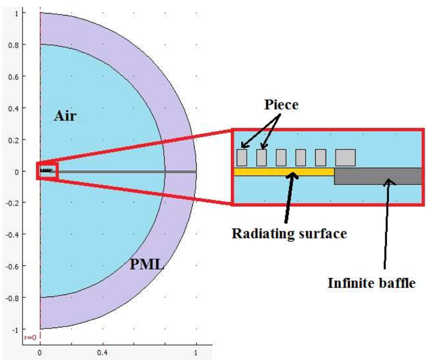


Figure 13 Zoomed simulation assembly conditions

Since the FEM and FDTD simulations confirm the experimental results obtained when measuring the frequency response in an anechoic chamber, we will only show the latter below while describing the experiment.

### 3.1. Thickness of polar piece

Figure 14 shows the frequency response of the loudspeaker variations when increasing the thickness of the pole piece (adding plates). The initial thickness was 10 mm and each plate added was 1 mm thick. This effect can be appreciated above 8.5 kHz. The phenomenon can be easily explained with a two-dimensional model.

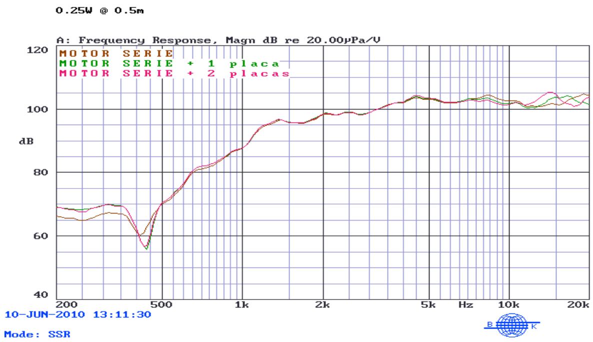


Figure 14 Effect of increasing front polar piece thickness

### 3.2. Bevels

Similarly, in the case of different bevel lengths and spacing, slight variations of the frequency response can be observed in the frequency response.

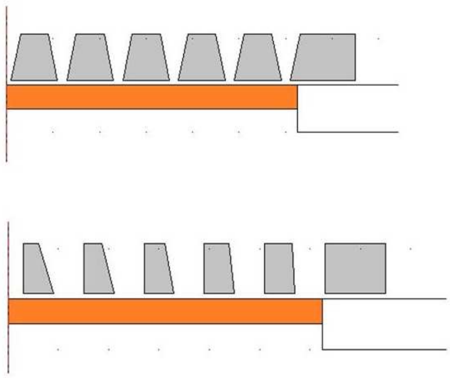

Figure 15 Different bevel geometries

Figure 16 shows a comparison of the frequency response in free field with and without bevel on the front pole piece. The effect, as in the previous case, is only significant at high frequency, where the figure has been zoomed for better viewing.

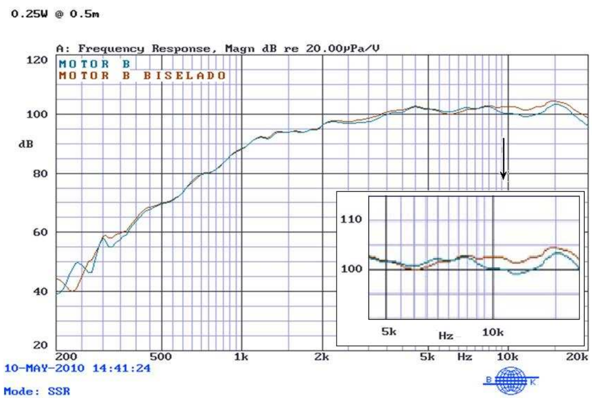


Figure 16 Effect of the bevel

## 4. CONCLUSIONS

We have presented a methodology to analyze the modal response of a structure composed of plate and cylindrical panels attached by their straight sides by using a simplification of the governing differential equations of the dynamic system. This approximation is valid when the length of the straight part is much greater than the radius of the cylindrical part. This condition is verified, i.e., in pleated moving assemblies of an AMT loudspeaker.

By assuming the hypothesis above, the components of the mode shapes can be written as a Levy type Fourier series, where the axial coordinate is the one to which series expansion is applied.

To test the analytical model implemented, a numerical experiment in FEM (using the software *Ansys*®) has been developed.

It is important to note that the analyzed structure is only one part of the moving assembly. In fact, in a real moving assembly we find this structure duplicated at least twenty times.

The first natural frequency of this structure obtained with this approach, for exciting harmonic loads corresponding to those of the loudspeaker performance, differ by less than 1% from that obtained in FEM with *Ansys*®. In addition, we saw a strong similarity in the w component. Finally, we should highlight its application to larger similar structures.

On the other hand we have presented experimental results about the acoustic polar piece contribution in the frequency response.

## 5. REFERENCES

[1] Colloms, M., Darlington, P., High performance loudspeakers, Willey, Michigan (2007)

[2] http://www.adamhall.com/uk/media/products/BY1/BY1TPL150-f2.pdf. Accessed on September, the 7th (2010)

[3] Martinez, J., Bolaños, F. Segovia Eulogio, E. and Ramis, J., Target modes in moving assemblies of a pleated loudspeaker, AES 127th Convention, 2009, October 9–12 New York, USA

[4] Segovia, E., Ferrer, B., Ramis, J.,Martinez, J. Modal behavior of a waveform structure composed of plates and cylindrical panels attached by their straight sides, International Methods for Numerical Methods in Engineering, Submitted on September (2010)

[5] A.A. Khdeir, J.N. Reddy & D. Frederick, A study of bending, vibration and buckling of cross-ply circular cylindrical shells with various shell theories. Int. J. Eng. Sci., Vol. 27 No. 11, pp. 1337-1359 (1989)

[6] Timoshenko & S. Woinowsky-Krieger, Theory of plates and shells, 2ºed., McGraw-Hill, New York (1959)

[7] J. George, Simitses & Ziqi Chen, Buckling of delaminated, long, cylindrical panels under pressure, Computers & Structures Vol. 28 No 2, pp. 173-184 (1988)

[8] A. Tafflove. Computational Electrodynamics: The Finite-Difference Time-Domain Method. Artech House Publishers,1995

[9] R. B. Wilson, M. Miller, P. K. Banerjee Free-vibration analysis of three-dimensional solids by BEM International Journal for Numerical Methods in Engineering, Vol 29(8), 1990.;1737-1757

[10] "ANSYS theory reference 8.1" ANSYS Inc., 2003